Derivative analysis of absorption features in hyperspectral remote sensing data of carbonate sediments

Eric M. Louchard, R. Pamela Reid, Carol F. Stephens
University of Miami,
Rosenstiel School of Marine and Atmospheric Science,
4600 Rickenbacker Causeway,
Miami, Florida, 33149
elouchard@rsmas.miami.edu, preid@rsmas.miami.edu,cstephens@rsmas.miami.edu

Curtiss O. Davis, Robert A. Leathers, T. Valerie Downes
Remote Sensing Division, Naval Research Laboratory,
4555 Overlook Ave. S.W.
Washington, DC 20375
curtiss.davis@nrl.navy.mil, leathers@nrl.navy.mil, downes@nrl.navy.mil

Robert Maffione
Hobi Labs
8987 E. Tanque Verde #309-366
Tucson, AZ 85749-9399, (520) 299-2589
maffione@hobilabs.com

Abstract: This study uses derivative spectroscopy to assess qualitative and quantitative information regarding seafloor types that can be extracted from hyperspectral remote sensing reflectance signals. Carbonate sediments with variable concentrations of microbial pigments were used as a model system. Reflectance signals measured directly over sediment bottoms were compared with remotely sensed data from the same sites collected using an airborne sensor. Absorption features associated with accessory pigments in the sediments were lost to the water column. However major sediment pigments, chlorophyll *a* and fucoxanthin, were identified in the remote sensing spectra and showed quantitative correlation with sediment pigment concentrations. Derivative spectra were also used to create a simple bathymetric algorithm.

©2002 Optical Society of America

OCIS code: (010.0010) Atmospheric and ocean optics

References and Links

1. W.L. Butler, and D.W. Hopkins, "Higher Derivative Analysis of Complex Absorption Spectra," Photochem. Photobiol. **12**, 439-450 (1970)
2. T.H., Demetriades-Shah, M.D. Steven, J.A. Clark, "High Resolution Derivative Spectra in Remote Sensing," Remote Sens. Environ. **33**, 55-64 (1990)
3. P.J. Curren, J.L., Dungan, B.A. Macler, S.E. Plummer, D.L. Peterson, "Reflectance Spectroscopy of Fresh Whole Leaves for the Estimation of Chemical Concentration," Remote Sens. Environ. **39**, 153-166 (1992)
4. A. Palacios-Orueta, and S.L. Ustin, "Remote Sensing of Soil Properties in the Santa Monica Mountains I. Spectral Analysis," Remote Sens. Environ, **65**, 170-183 (1998)

#1802 - $15.00 US Received November 06, 2002; Revised December 23, 2002
(C) 2002 OSA

5. E.M. Rollin, and E.J. Milton, "Processing of High Spectral Resolution Reflectance Data for the Retrieval of Canopy Water Content Information." Remote Sens. Environ. **65**, 86-92 (1998)
6. R.F. Kokaly, and R.N. Clark, "Spectroscopic Determination of Leaf Biochemistry Using Band-Depth Analysis of Absorption Features and Stepwise Multiple Linear Regression," Remote Sens. Environ. **67**, 267-287 (1999)
7. R.C. Zimmerman, and S.K. Wittlinger, "Hyperspectral remote sensing of submerged aquatic vegetation in optically shallow waters," In S.G. Ackleson [ed.], Ocean Optics XV. CD-ROM Proc. paper no.1138, 6. (2000)
8. R.C. Smith, and K.S. Baker, "Optical properties of the clearest natural waters (200-800 nm)," App. Opt., **20**, 177-184 (1981)
9. C.F. Stephens, E.M. Louchard, R.P. Reid, R.A. Maffione, "Effects of microalgal communities on reflectance spectra of carbonate sediments in subtidal optically shallow marine environments," Limnol. Oceanogr. Special Issue: Shallow Water Optics. in press.
10. E.M. Louchard "Spectral reflectance of carbonate sediments and application to shallow water benthic habitat classification," Doctoral Dissertation, University of Miami. Chap.3, (2003)
11. R. Dill, "Subtidal stromatolites, ooids and crusted line-muds at the Great Bahama Bank margin," Society for Sedimentary Geology, SEPM Special Publication No. 46, pp.147-171 (1991)
12. C.O. Davis, J. Bowles, R.A. Leathers, D. Korwan, T.V. Downes, W.A. Snyder, W.J. Rhea, W. Chen, J. Fisher, W.P. Bissett, R.A. Reisse, "Ocean PHILLS hyperspectral imager: design, characterization, and calibration," Opt. Express. **10**, 210—221 (2002) http://www.opticsexpress.org/abstract/.cfm?URI=OPEX-10-4-210
13. R.M. Pope, E.S. Fry, "Absorption spectrum (380-700 nm) of pure water. II. Integrating cavity measurements," Appl. Opt. **36**, 8710-8723 (1997)
14. F. Tsai, and W. Philpot, "Derivative analysis of Hyperspectral Data," Remote Sens. Environ. **66**, 41-51 (1998)
15. R.L. Huguenin, and J.L. Jones, "Intelligent Information Extraction from Reflectance Spectra: Absorption band Position," J. Geophys. Res. **91**, 9585-9598 (1986)
16. N. Hoepffner, and S. Sathyendranath, "Effect of pigment composition on absorption properties of phytoplankton," Mar. Ecol. Prog. Ser. **73**, 11-23 (1991)
17. S.W. Jeffrey, R.F.C. Mantoura, S.W. Wright, *Phytoplankton pigments in oceanography: guidelines to modern methods* (Unesco Publishing, 1997), Chap. 4.
18. C.K.N. Tam, & A.C. Patel, "Optical absorption coefficients of water," Nature. **280**, 302-304 (1979)

1. Introduction

Derivative spectroscopy is a powerful tool that is commonly used in the analysis of hyperspectral remote sensing data from terrestrial environments. Derivative techniques enhance minute fluctuations in reflectance spectra and separate closely related absorption features. Analytical chemists working in remote sensing have, for example, used derivative spectroscopy for many years to eliminate background signal and to resolve overlapping features. A primary application has been to analyze pigment and chemical composition of leaves in order to track physiological changes in plant canopies [1-6].

Increasing use of hyperspectral sensors for marine remote sensing opens the possibility of using derivative techniques for studies of the benthos in coastal environments (*e.g.,* Ref. 7). Remote sensing studies in shallow marine environments are significantly more complex, however, than their terrestrial counterparts. Reflectance from the seafloor must be transmitted through a column of water, which attenuates light in a wavelength-dependent manner, changing both its color and intensity [8]. In this paper, we use derivative spectroscopy to enhance and compare absorption features in reflectance signals collected on the sea floor and in the atmosphere to assess losses in qualitative and quantitative spectral information incurred by the water column.

Carbonate sediments are an ideal model system for investigating water column transmission of detailed spectral information regarding benthic substrates. Sediments have relatively homogeneous distribution and thus avoid problems of pixel mixing associated with remote sensing of heterogeneous bottom types, such as coral reefs. Moreover, Stephens and colleagues have shown that detailed information on the structure and composition of microbial communities in carbonate sediments is contained in bottom reflectance spectra (9). The goal of the present research is to determine if this type of detailed benthic information is

#1802 - $15.00 US Received November 06, 2002; Revised December 23, 2002
(C) 2002 OSA

retained when bottom reflectance spectra are transmitted through the water column. A clear understanding of the effects of water column attenuation on benthic reflectance signals will be important in creating analytical models for seafloor mapping using data from a variety of remote sensing platforms.

2. Methods

2.1 Field Site and Sediment Description

The study site for this research was Lee Stocking Island (LSI), Bahamas, a region characterized by carbonate sediments and clear shallow water. Six carbonate sediment types, representing distinct sedimentary environments, were recognized in the vicinity of LSI (Fig. 1); site locations were recorded using GPS. Each sediment type was described based on pigment content (Table 1) measured using High-Performance Liquid Chromatography (HPLC) on sediment cores (see Stephens et al. [9] for methodology of sediment pigment analysis). Sediment pigments have a major effect on both the shape and magnitude of spectral reflectance [9]. Other factors, such as grain size and shape, can affect spectral magnitude but these textural parameters were relatively constant between the different field sites at LSI [10]. Sediment types were categorized into three major groups depending on the amount of microbial film present: minimal microbial film (Sediment Types 1,2); moderate microbial film (Sediment Types 3,4); dense microbial film (Sediment Types 5,6).

Analysis of the bottom sediments using HPLC identified a variety of pigments including chlorophyll *a* and *b*, xanthophylls (fucoxanthin, peridinin) and carotenoids (zeaxanthin, lutein, *B*-carotene) [9]. Water depth ranged from 1.5 m to 7 m over most of the sediment bottoms, except for Sediment Type 6, at 16 m depth.

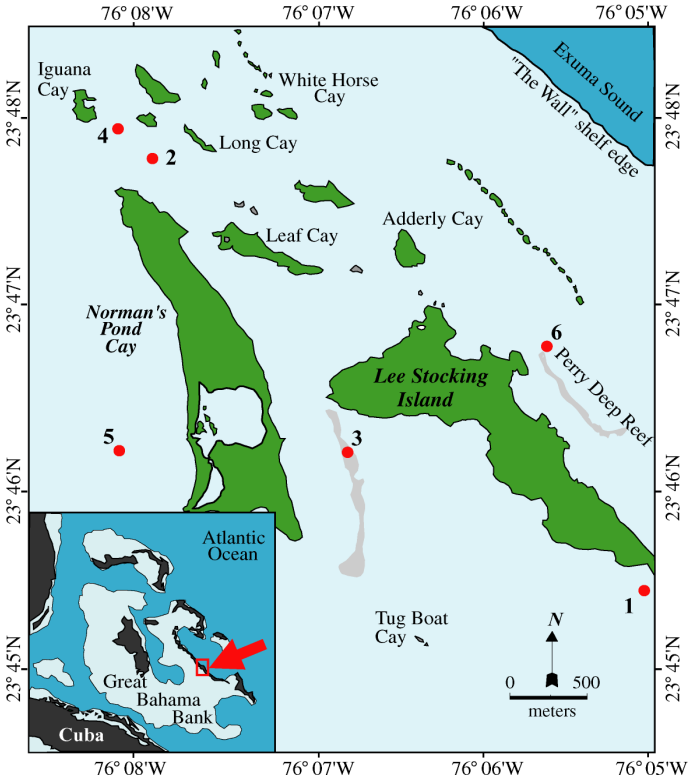

Fig. 1. Map of Lee Stocking Island (after [11]) showing the locations of the six sediment sampling sites.

#1802 - $15.00 US
Received November 06, 2002; Revised December 23, 2002
(C) 2002 OSA

Table 1. Sediment types and mean pigment composition in μg g^{-1}. Pigments identified by abbreviation: Chl *a* = chlorophyll *a*; Chlide *a* = chlorophillide *a*; Chl *b* = chlorophyll *b*; Fuc = fucoxanthin; Per = peridinin; But = 19'-Butanoloxyfucoxanthin; Zea = zeaxanthin; Lut = lutein; β-Car = β carotene. ND = Not Detected.

Sed. Type.	Depth (m)	Chl *a*+Chlide *a*	Chl b	Fuc	Per	But	Zea	Lut	β-Car
1	1.5	0.84±0.43	ND	0.48±0.26	0.05±03	ND	0.06±0.01	0.02±0.02	0.02±0.01
2	2.5	0.43±1.06	ND	0.07-1.38	ND	ND	0.06-0.74	ND	ND
3	2.5	1.55±1.36	ND	0.01±0.01	ND	ND	0.22±0.02	ND	0.14±0.04
4	7.0	1.45±0.53	0.04±0.02	0.64±0.21	0.10±0.06	ND	0.11±0.04	0.02±0.01	0.03±0.02
5	2.0	12.56±2.54	0.10±0.10	4.71±0.56	0.01±0.01	0.12±0.10	0.48±0.09	0.08±0.03	0.44±0.11
6	16.0	17.08±6.44	0.11±0.15	7.24±2.43	0.06±0.07	0.06±0.03	0.57±0.22	0.13±0.09	0.59±0.27

2.2 Sediment reflectance

The primary methodology used to measure spectral reflectance of sediments was a newly developed core technique. Ten sediment cores (22 mm diameter, 100 mm length) were taken with random spacing at each sampling site in a 0.25 m^2 area, delineated with a square made of plastic piping, and returned to the laboratory for analysis. Reflectance spectra were measured by placing a core tube in a custom-designed holder constructed from a solid plastic cylinder, which was cut into a hollow shell. A hole in the top of the cylinder allowed an Ocean Optics RP200-7 Reflection Probe to be held at 0° to the sediment surface. An Ocean Optics S2000 UV-VIS spectrometer (grid#2, 50 μm slit) was connected to the RP200-7 by a 200 μm fiberoptic cable and co-joined to an Ocean Optics LS-1 tungsten halogen light source. Reflectance spectra were measured for wavelengths ranging from 190 nm to 890 nm in 2048 channels (approximately 0.30 nm bandwidth).

A reference spectrum was collected using an Ocean Optics WS-1 99% Spectralon disk, held in a PVC cylinder similar to the cylinder used for the sediment cores. The RP200-7 probe was clamped at a constant 25 mm distance normal to the WS-1 surface and the cylinder was filled with filtered seawater. Micro-bubbles on the target surface were removed with seawater squirted from a plastic pipette. The LS-1 lamp and S2000 were warmed up while viewing the WS-1 standard until measurements stabilized. Once the spectrometer stabilized, ten measurements of spectrometer counts under illumination (CR_L) and in darkness (CR_D) were made.

Light reflected from the sediment was measured as spectrometer counts (CS_L) three times for each sediment core, rotating the core 120° between measurements. Sediments were kept submerged in seawater during measurement. Dark current (CS_D) was measured once for each set of ten cores by taking three measurements of one core with the lamp off. This procedure reduced stress resulting from cycling the lamp on and off. Radiance reflectance was calculated as follows:

$$R = 0.99\left(\frac{CS_L - CS_D}{CR_L - CR_D}\right)\left(\frac{\text{int}_R}{\text{int}_S}\right) \quad (1)$$

CS_L and CS_D are the mean spectrometer counts measured for the sample in light and dark, respectively. The variables int_S and int_R are the sample and reference standard integration times and CR_L and CR_D are the mean spectrometer counts measured for the WS-1 reference standard in light and dark, respectively.

S2000 spectrometer data were smoothed and binned into 5 nm wide bands using a cubic spline function. This was necessary in order to match the S2000 resolution to the resolution of remote sensing data. Cubic splines also provided the added benefit of replacing the irregularly spaced S2000 data with evenly spaced data.

#1802 - $15.00 US Received November 06, 2002; Revised December 23, 2002
(C) 2002 OSA

2.3 Airborne remote sensing imagery

Hyperspectral images of remote sensing reflectance (R_{rs}) LSI (Fig. 2) were collected as part of ONR's project on Coastal Benthic Optical Properties (CoBOP). Images were collected using an airborne version of the Portable Hyperspectral Imager for Low Light Spectroscopy (PHILLS) sensor, a system designed specifically for shallow coastal water remote sensing [12]. The composite PHILLS image was georeferenced using ground control points from IKONOS multispectral imagery of the Lee Stocking Island area. Radiometric calibration and atmospheric correction of the PHILLS system was performed following Davis et al. [12]. with additional atmospheric correction involving subtraction of the R_{rs} spectrum of an offshore deep-water pixel from the R_{rs} spectra of all pixels in the image.

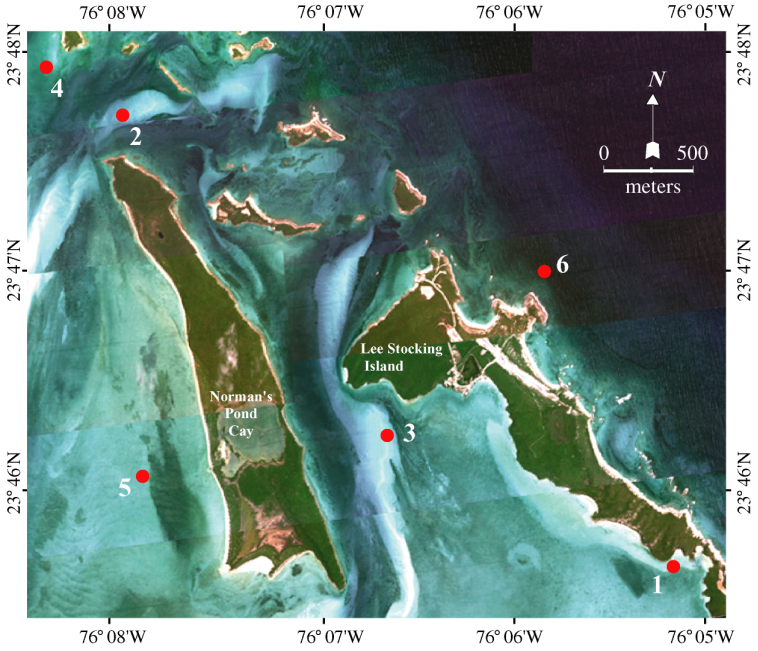

Fig. 2. Airborne PHILLS image of Lee Stocking Island and Norman's Pond Cay. Sediment sampling sites are shown in red. The image is a false color mosaic of several flight lines.

The PHILLS system was carried on an Antonov AN-2 biplane, traveling at a cruising speed of 45 m s^{-1} and at an altitude of 2360 m. The PHILLS camera produced images with a 1.25 m x 1.25 m Ground Sample Distance (GSD) pixel size and 1.25 km swath. Hyperspectral values of R_{rs} were collected in 69 spectral channels, ranging from 400-700 nm.

PHILLS imagery used for the present study was acquired between 9:30 and 10:30am EST on 01 June 1999, when the solar zenith angle was close to 30°. Ship reports indicated low wind (2 m s^{-1}), minimal ocean swell, and clear skies.

Pixels for spectral analysis were located on the georeferenced PHILLS image using the GPS position of the sediment sampling sites and extracted using the program ENVI (Research System Inc. Boulder, CO). PHILLS R_{rs} spectra were binned into 5 nm spaced bands using a cubic spline function to reduce noise and to match S2000 data. Spectral shape was retained through the use of the maximum number of nodes for the data points.

2.4 Water Column Optical Properties

In optically shallow waters, R_{rs} spectra are affected by absorption and scattering from both the bottom and the water column. Attenuation effects caused by the water column alone were

#1802 - $15.00 US
Received November 06, 2002; Revised December 23, 2002
(C) 2002 OSA

analyzed using PHILLS data from a region of optically deep water, where the bottom did not affect the remote sensing signal. The deep water R_{rs} spectrum includes the combined absorption effects of water, phytoplankton, suspended sediments, and dissolved organic material in the water column. Reflectance of pure water was analyzed using the absorption (*a*) and scattering (*b*) spectra measured by Pope and Fry [13] to create a beam attenuation spectrum ($c=a+b$); this spectrum was inverted (1 minus *c*) to appear as a pseudo "reflectance" for empirical comparisons with sediment reflectance.

2.5 Derivative analysis

Absorption features in reflectance spectra were enhanced using derivative spectroscopy. The process of creating derivative spectra proceeded using finite approximation to calculate the change in reflectance over a bandwidth $\Delta\lambda$, defined as $\Delta\lambda = \lambda_j - \lambda_i$, where $\lambda_j > \lambda_i$ [14]. The estimation for the first derivative is shown in Eq. 2. The nth derivative was computed using Eq. 3.

$$\left.\frac{\mathrm{d}s}{\mathrm{d}\lambda}\right|_i \approx \frac{s(\lambda_i) - s(\lambda_j)}{\Delta\lambda} \tag{2}$$

$$\left.\frac{\mathrm{d}^n s}{\mathrm{d}\lambda^n}\right|_j = \frac{d}{d\lambda}\left(\frac{d^{(n-1)}s}{d\lambda^{(n-1)}}\right) \tag{3}$$

Calculations of derivative spectra followed the same processes for reflectance data from the S2000 spectrometer, R_{rs} spectra from the PHILLS airborne sensor, and the "reflectance" spectrum of pure water. A bandwidth ($\Delta\lambda$) was selected for each data type to maximize the signal to noise amplification ratio. A bandwidth of 15 nm (3 points) was found to be optimal for S2000 and PHILLS data whereas 30 nm (3 points) was optimal for pure water.

Peaks in the derivative spectra were distinguished from spectrometer noise using the method of Huguenin and Jones [15]. Positive peaks in the second derivative spectra were examined in the fourth and fifth derivative spectra. If the magnitude of the peak was negative in the fourth derivative and equal to zero in the fifth derivative, then the peak was classified as an absorption feature and was not noise related.

Derivative spectra were use in both qualitative and quantitative analysis of microbial pigments in the sediments. Qualitative information regarding pigment composition was obtained based on the wavelength position of absorption features in derivative spectra. Absorption features were compared with published values of the wavelength positions of pigment absorption peaks. We also explored use of second derivative peaks for quantitative estimations of microbial pigment concentrations in the sediment biofilms. Previous research has illustrated the effectiveness of derivative techniques for estimating pigment concentrations using S2000 data [9]. In the present study, peaks in the PHILLS derivative spectra were compared to pigment concentrations measured at each sampling site to determine if quantitative information is retained in remote sensing measurements.

3. Results and Discussion

3.1 Spectral Reflectance

Reflectance spectra measured from sediment cores using the S2000 spectrometer displayed a high degree of variation in magnitude and shape between sediment types (Fig. 4A). Reflectance magnitude was highest in sediment with minimal microbial components (Sediment Types 1,2) and lowest in sediments with dense microbial layers (Sediment Types 5,6). Reflectance values in all the sediment spectra decreased between 550-400 nm (Fig. 4A). This decrease in magnitude in low wavelengths contrasted with the pseudo "reflectance" of

#1802 - $15.00 US Received November 06, 2002; Revised December 23, 2002
(C) 2002 OSA

pure water, which is high in wavelengths 400-550 nm and drops rapidly past 600 nm (Fig. 4B).

The magnitude and shape of reflectance signals collected using the airborne PHILLS sensor (Fig. 4C) differ significantly from the S2000 seafloor measurements (Fig. 4A). The remote sensing reflectance spectra show a sharp decline in reflectance past 600 nm (Fig. 4C), corresponding to increased attenuation in this region in the pure water spectrum (Fig. 4B). The overall magnitude of PHILLS R_{rs} data was also reduced by an order of magnitude when compared with S2000 data, with lower magnitudes corresponding to sites at greater depths. However, even at the deepest sampling site (Sediment Type 6), Rrs was higher than the deep water measurement (Fig. 4C), indicating that the bottom affected the signal at depths at least as great as 16m.

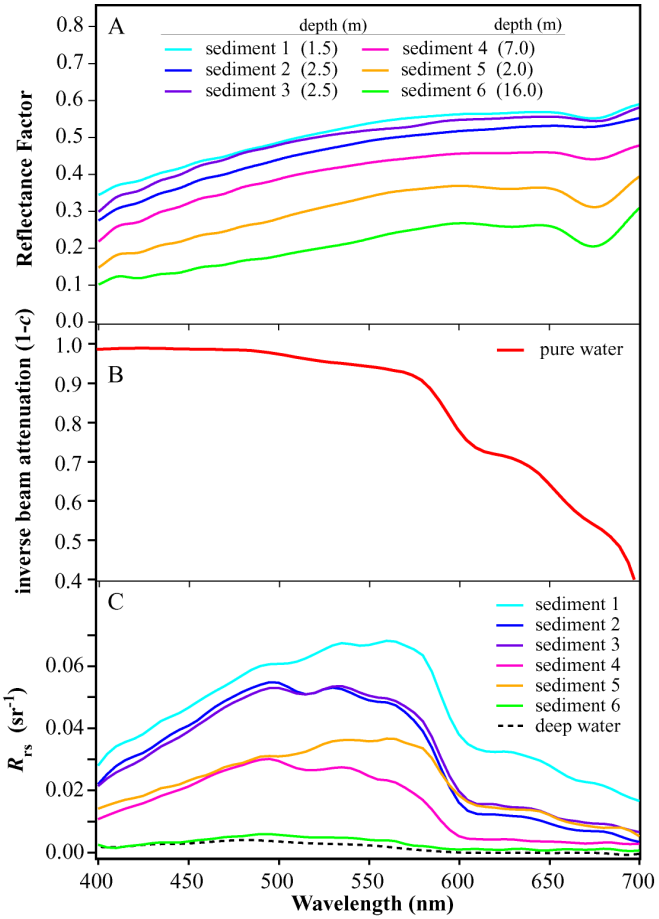

Fig. 4. Reflectance spectra. (A) Bottom reflectance measured on sediment cores using an S2000 spectrometer. (B) Pure water pseudo "reflectance" from inverse of beam attenuation coefficient. (C) Remote sensing reflectance measured with a PHILLS airborne sensor over sediment sampling sites and deep water.

3.2 Qualitative Derivative Analysis

Derivative spectroscopy was used to extract qualitative information regarding pigment composition by enhancing fine scale absorption features. S2000 derivative spectra (Fig. 5A) were compared with derivative spectra of pure water (Fig. 5B) and PHILLS data (Fig. 5C) to examine the effects of water column attenuation, as discussed below.

#1802 - $15.00 US
Received November 06, 2002; Revised December 23, 2002
(C) 2002 OSA

S2000 derivative spectra (Fig. 5A) revealed 11 sharp features relating to chlorophyll *a*, its degradation product chlorophyllide *a*, and a variety of accessory pigments (Table 2A). The most consistent and largest absorption feature for chlorophyll *a* and chlorophyllide *a* was located at 680 nm (Peak 11, Fig. 5A). Two other prominent chlorophyll and chlorophyllide *a* absorption features were located at 425 nm and 445 nm (Peaks 1&2, Fig. 5A) in all samples. Chlorophyll *b* was identified in the derivative spectra at 470 nm (Peak 3, Fig. 5A) but this absorption feature was not consistently present in all samples. Minor absorption features relating to chlorophylls *a* and *c* were also found at 575 nm and 585 nm (Peaks 7&8, Fig. 5A) [9]. An absorption feature for numerous carotenoids, such as β-carotene and lutein was identified at 495 nm (Peak 4, Fig. 5A) but the overlap of multiple absorption features prevented further separation of pigments. An important feature at 540 nm (Peak 6, Fig. 5A) indicated absorption by fucoxanthin, a pigment found primarily in benthic diatoms [9,16]. A second minor absorption feature relating to fucoxanthin was found at 515 nm (Peak 5, Fig. 5A). Other xanthophylls, peridinin and 19'-butanoloxyfucoxanthin, also absorb at 540 nm and 515 nm, but HPLC analyses indicating low levels of these pigments in the sediments (Table 1) suggest that the peak at 515 nm is primarily due to fucoxanthin absorption. A final absorption feature was observed at 630 nm, in a region associated with the biliprotein, phycocyanin [16,17]. As biliproteins are water soluble, they were not detected in HPLC data.

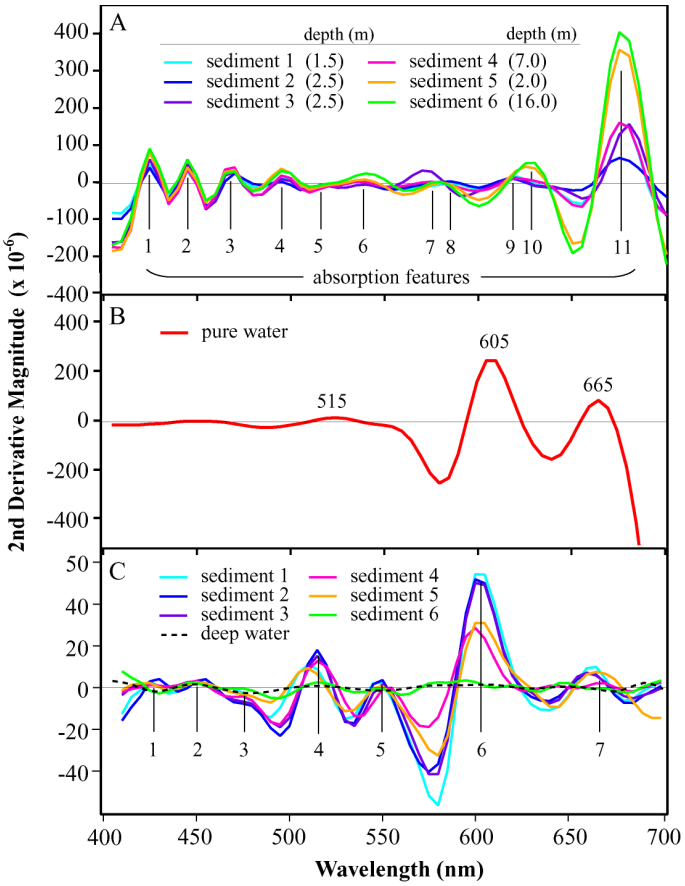

Fig. 5. Second derivative of reflectance spectra. (A) Absorption features in sediment core reflectance measured with the S2000 spectrometer. (B) Absorption features in pure water pseudo "reflectance", calculated as from the inverse of beam attenuation coefficient. (C) Absorption features in remote sensing reflectance measured with the PHILLS airborne sensor over the sediment sampling sites and deep water.

#1802 - $15.00 US
Received November 06, 2002; Revised December 23, 2002
(C) 2002 OSA

Table 2. Wavelength positions (nm) of absorption features identified in derivative spectra. Pigment abbreviations: Chl *a* = chlorophyll *a*; Chl *b* = chlorophyll *b*; Chl *c* = chlorophyll *c*; Fuc = fucoxanthin; Per = peridinin; But = 19'-Butanoloxyfucoxanthin; Zea = zeaxanthin; Lut = lutein; β-Car = β carotene; Phy = Phycocyanin.

A. S2000 Spectrometer

		Sediment Type					
Der. Peak	Pigment	1	2	3	4	5	6
1	Chl *a*	425	425	425	425	425	425
2	Chl *a*	445	445	445	445	445	445
3	Chl *b*	470	470	470	470	470	470
4	Lut/β Car/Zea	495	495	495	495	495	495
5	Fuc/Per/But	515	520	520	520	520	515
6	Fuc/Per/ But	530	535	540	535	540	540
7	Chl *a*/ Chl *c*			575	575		
8	Chl *a*/ Chl *c*	585	585			585	585
9	Phy	620	620	620	620		
10	Phy					630	630
11	Chl *a*	680	680	680	680	680	680

B. PHILLS

		Sediment Type						Deep
Der. Peak	Pigment	1	2	3	4	5	6	Water
1	Chl *a*	425	430	425	425	420	425	
2	Chl *a*	450	455	450	450	445	450	450
3	Chl *b*	470	475	480	475	475	475	
4	Water (Fuc/Per/But	510	515	515	515	515	510	515
5	Fuc/Per/But	545	550	550	555	550	550	
6	Water	605	605	605	605	600	605	605
7	Water	665	660	660	670		665	685(650)

Derivative analysis of the inverse beam attenuation spectrum of pure water identified three major absorption features at 515 nm, 605 nm, and 665 nm (Fig. 5B); the peaks at 515 and 605 nm are located at the shoulders of peaks in the absorption coefficient caused by harmonics of the O-H stretch vibration of water molecules [18]. Peaks related to scattering were not observed in the pure water spectrum as scattering is a minor factor in the beam attenuation coefficient.

Derivative spectra created from PHILLS R_{rs} data show a combination of absorption features related to pure water and pigments. Absorption features of pure water were prominent in PHILLS R_{rs} spectra at 510-515 nm, 600-605 nm, and 660-670 nm (Peaks 4,6,9, Fig. 5C). Pigment absorption features were found in the wavelength range of 400-550 nm (Table 2B), where pure water absorption was lowest (Fig. 5B). Peaks locations are indicative of chlorophyll *a* and chlorophyllide *a* (420-430 nm, 445-460 nm) and chlorophyll *b* (470-480 nm) (Peaks 1,2&3, Fig. 5C). Chlorophyll *a* and chlorophyllide *a* could not be separated as their absorption spectra overlapped. An absorption feature related to fucoxanthin and peridinin was located at 550-555 nm (Peak 5, Fig. 5C); this peak is shifted in wavelength position with respect to S2000 data, where it occurs at 535-540 nm (Peak 6, Fig. 5A). The shifts are likely caused by pure water absorption centered at 510-515 nm and 600-605 nm, which reduces R_{rs} at the shoulders of the dip normally found at approximately 540 nm. The higher rate of flattening of the shoulder at 600-605 nm, due to higher absorption coefficient, has the effect of shifting the minimum point at the base of the dip (2^{nd} derivative maximum) 10-15 nm to the red.

As PHILLS R_{rs} spectra data from the sampling sites are affected by pigments in the water column as well as the sediments it is necessary to isolate the effects of each. Derivative analysis of the deep water reflectance spectrum provides an indication of the relative contributions of the water column versus the bottom in the PHILLS R_{rs} data. Analysis of the deep water R_{rs} spectrum identified three absorption features at 450 nm, 515 nm and 605 nm (Table 2B; Peaks 2,4,6, Fig. 5C). The 450 nm peak, which represents chlorophyll *a*

#1802 - $15.00 US Received November 06, 2002; Revised December 23, 2002
(C) 2002 OSA

absorption, is likely caused by phytoplankton in the water column. The lack of absorption features, however, for chlorophyll a at 420 nm and chlorophyll b at 475 nm (Peaks 1&3, Fig. 5C) suggests that phytoplankton pigments in the water column were a negligible component of the remote sensing signal. The other absorption features, at 515 nm and 605 nm, in the deep water spectrum are caused by water. A third water absorption feature, found at 665 nm in pure water (Fig. 5B), was split up by noise into two peaks at 650 nm and 685 nm in the deep water spectrum (Peak 7 Fig. 5C).

3.3 Quantitative Derivative Analysis

Further analyses of PHILLS R_{rs} derivative spectra revealed that information regarding pigment concentrations in the bottom sediments could be extracted from remote sensing reflectance data. Derivative analysis was effective for quantitative estimates of total microbial biomass (chlorophyll *a* + chlorophyllide *a*) and xanthophyll concentration (fucoxanthin + peridinin + 19'-butanoloxyfucoxanthin). A good correlation and linear regression (R^2 = 0.951) was found between the sum of chlorophyll *a* and chlorophyllide *a* verses the ratio of the 2nd derivative peak magnitudes at 450 nm and 515 nm. The peak at 515 nm was used to normalize for water depth (Fig. 6A). A similar relationship (R^2 = 0.935) was found between xanthophyll concentrations and the ratio of 2nd derivative peak magnitude at 550 nm verses the square of the 2nd derivative peak at 515 nm (Fig. 6B). This relationship is primarily an indication of fucoxanthin abundance, as concentrations of peridinin and 19'-butanoloxyfucoxanthin are very low in these sediments (Table 1).

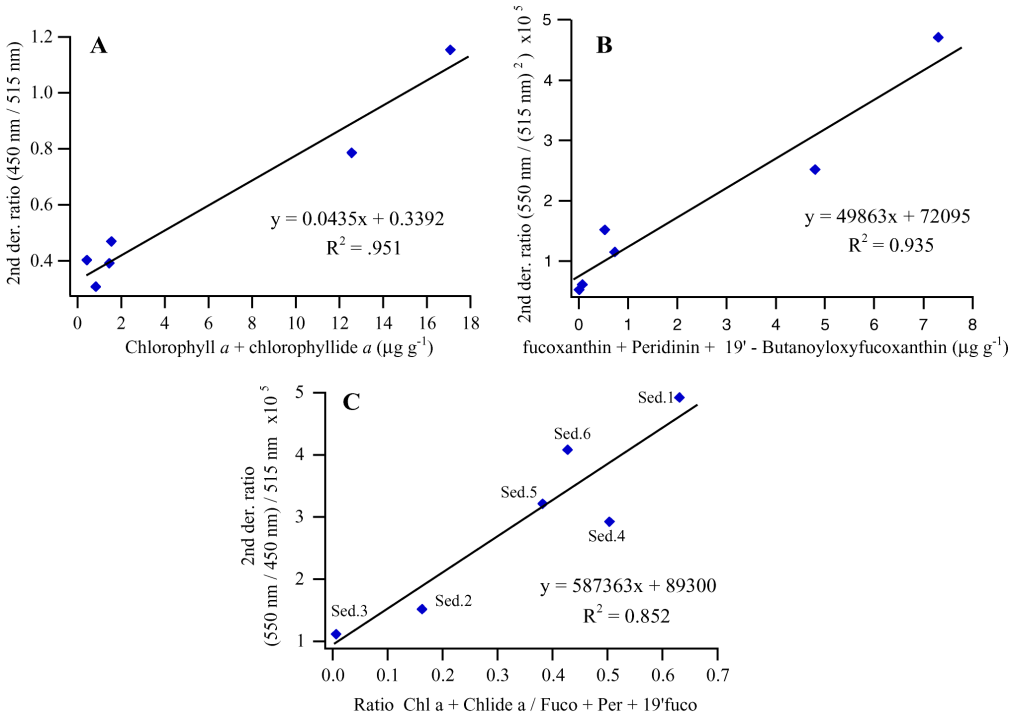

Fig. 6. Quantitative relationships between sediment pigment concentrations, as determined from HPLC, and derivative peak heights. A) Linear regression of the ratio of 2nd derivative magnitude at 444 nm and 515 nm verses total biomass (chlorophyll *a* and chlorophyllide *a*). B) Linear regression of the ratio of 2nd derivative magnitude at 550 nm and 515 nm squared verses xanthophyll concentration (fucoxanthin + peridinin +19'-butanoloxyfucoxanthin). C) Linear regression of the ratio of 2nd derivative magnitude (550 nm / 450 nm) / (515 nm) verses the ratio of total biomass and xanthophyll concentration.

#1802 - $15.00 US Received November 06, 2002; Revised December 23, 2002
(C) 2002 OSA

Successful estimation of pigment concentrations through derivative spectroscopy allows for differentiation of sediment types with distinct microbial community structures. For example, Sediment Types 2 and 3 have low ratios of fucoxanthin verses chlorophyll *a* (Table 1), indicating low concentrations of diatoms. These sediment types were located in high-energy sites, where strong tidal currents inhibit development of diatom films on the sediments; the primary microbial components at these sites are endolithic cyanobacteria, which bore into the carbonate grains [9]. To ascertain if these differences in pigment ratios could be detected in remote sensing spectra, derivative peaks for chlorophyll *a* and fucoxanthin found above were compared to the ratio of those pigments in sediment. A good correlation and linear regression (R^2 = 0.852) was found between the ratio of pigments (chlorophyll *a* + chlorophyllide *a*) / (fucoxanthin + peridinin + 19'-butanoloxyfucoxanthin) verses the ratio of the 2nd derivative peak magnitudes (550 nm / 450 nm) / (515 nm). Although the accessory pigments peridinin+19'-butanoloxyfucoxanthin were included in the calculations, chlorophyll *a* and fucoxanthin were the primary pigments determining the relationships as these have the highest concentrations in HPLC (Table 1).

A potential problem with estimating sediment pigment concentrations using derivative peak heights is that microbial pigments in the sediment absorb at the same wavelengths as pigments in the water column. As a result, waters with high levels of phytoplankton could effectively mask seafloor pigments. At LSI, derivative peaks show a good correlation with sediment pigment concentrations (Fig. 6A, 6B) because the effects of phytoplankton, suspended sediment, and dissolved organic matter on remote sensing reflectance were minor compared to seafloor reflectance. The relationships in Fig. 6 may not apply if water column phytoplantkon were more abundant and/or sediment microbes less abundant than at LSI. An effective approach in using remote sensing data for analysis of benthic information would be to remove the effects of the water column from R_{rs} spectra using radiative transfer simulations to recover bottom reflectance. This would improve derivative analysis by recovering both spectral shape information, which creates peaks in the derivative spectra, and magnitude information, which determines the height of the derivative peaks used in estimating sediment pigment concentrations.

3.4 Bathymetric Estimation

An additional application of the PHILLS derivative spectra is estimation of water depth over shallow carbonate sediments. A good correlation with depth was achieved (R^2 = 0.9524) after taking the ratio of the magnitude of the 2nd derivative peak at 605 nm verses 515 nm and comparing the ratio to water depth (Fig. 7).

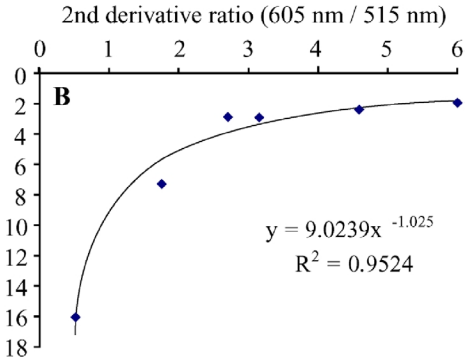

Fig. 7. Bathymetric algorithm using ratio of derivative peak magnitudes from PHILLS data. The algorithm uses the ratio of second derivative magnitude at 605 nm divided by 515 nm verses water depth.

#1802 - $15.00 US Received November 06, 2002; Revised December 23, 2002
(C) 2002 OSA

It should be noted that this algorithm is specific for bathymetric estimation over shallow carbonate sediment bottoms. The derivative peaks utilized in the algorithm depend on the shape of the bottom reflectance and may not be applicable over different bottom types, such as seagrass or coral. Additional studies would be needed to expand the methodology to estimate water depth over an entire hyperspectral image with variable bottom types. One approach might be to use indicator wavelengths or spatial analysis to group pixels into major bottom types, such as coral, seagrass, or sediment, then apply different derivative bathymetry algorithms for each bottom type. The algorithm would also need to be modified for regions with different concentrations of phytoplankton, colored dissolved organic matter, or suspended sediments, which alter the inherent optical properties of the water column.

4. Conclusions

Our results indicate that derivative analysis of hyperspectral remote sensing data is a potentially powerful method for detailed analysis of benthic substrates. As in terrestrial systems, derivative analysis of shallow marine hyperspectral data provides a method for quickly identifying spectral absorption features, thereby simplifying large numerical data sets into smaller, more manageable units. These absorption features can be used to extract detailed qualitative and quantitative information about benthic substrates.

In this study, derivative analysis of remote sensing data collected by an airborne hyperspectral sensor showed that a number of subtleties in the bottom reflectance spectra of carbonate sediments were propagated through the water column. Although information on minor microbial components of the sediment was lost to the water column, remotely sensed spectra contained qualitative and quantitative information on major sediment pigments, such as chlorophyll *a* and fucoxanthin. Derivative analysis of spectral absorption features was effective for identifying microbial pigments and pigment concentrations were successfully estimated using derivative peak magnitudes. Development of techniques to remove the effects of water column attenuation, in the same way that corrections are currently made for atmospheric absorption and scattering, could greatly improve our ability to extract relevant information on benthic substrates from marine remote sensing data.

In addition to providing qualitative and quantitative information regarding seafloor type, derivative analysis can also be useful for estimation of bathymetry. The wavelength-dependent changes in reflectance caused by water absorption, which modify spectral slope, result in changes in 2^{nd} derivative peak magnitudes that are dependent on depth. The magnitude of derivative peaks can therefore be used in estimations of bathymetry. Future development of robust bathymetric algorithms will be of critical importance for modeling and classifying shallow marine habitats

Acknowledgements

This work was supported by the Office of Naval Research Environmental Optics program Awards # N000149710010 and N00149910130. We thank Howard Gordon and Emmanuel Boss for discussion on optical theory; Jeffrey Bowles, Mary Kappus, Megan Carney, and Bosch Aerospace Inc. for PHILLS data collection; and other members of the CoBOP program and the staff of the Caribbean Marine Research Center at Lee Stocking Island, Bahamas for additional field assistance. Constructive comments from three anonymous reviewers of Optics Express were greatly appreciated.